Mon. Not. R. Astron. Soc. **000**, 000–000 (0000) Printed 4 July 2013 (MN LATEX style file v2.2)

Variability of M giant stars based on *Kepler* photometry: general characteristics

E. Bányai[1], L. L. Kiss[1,2,3], T. R. Bedding[2], J. M. Benkő[1], A. Bódi[4], J. Callingham[2], D. Compton[2], I. Csányi[4], A. Derekas[1,2], J. Dorval[2], D. Huber[2,5], A. E. Simon[1,3], D. Stello[2], Gy. M. Szabó[1,3,4], R. Szabó[1], K. Szatmáry[4]

[1]*Konkoly Observatory, Research Centre for Astronomy and Earth Sciences, Hungarian Academy of Sciences, H-1121 Budapest, Konkoly Thege M. út 15-17, Hungary*

[2]*Sydney Institute for Astronomy (SIfA), School of Physics, The University of Sydney, NSW 2006, Australia*

[3]*ELTE Gothard-Lendület Research Group, H-9700 Szombathely, Szent Imre herceg út 112, Hungary*

[4]*Department of Experimental Physics and Astronomical Observatory, University of Szeged, H-6720 Szeged, Dóm tér 9., Hungary*

[5]*NASA Ames Research Center, Moffett Field, CA 94035, USA*

Accepted ... Received ..; in original form ..

ABSTRACT

M giants are among the longest-period pulsating stars, surpassed only by the more luminous supergiant red stars. These long periods have meant that studies of these stars have traditionally been restricted to analyses of many decades of low-precision visual observations, or more recently, accurate ground-based CCD photometric data. Here we present an overview of M giant variability on a wide range of time-scales (hours to years), based on analysis of thirteen quarters of *Kepler* long-cadence observations (one point per every 29.4 minutes), with a total time-span of over 1000 days. About two-thirds of our sample stars have initially been selected from the ASAS-North survey of the *Kepler* field, hence being a variability selected sample and supplemented with a randomly chosen M giant control sample.

We first describe issues concerning the correction of the light curves from different quarters, which is essential for studying the slowly varying M giants in *Kepler* data. We use Fourier analysis to calculate multiple frequencies for all stars in the sample. Over 50 objects show a relatively strong signal with a period equal to the Kepler-year and a characteristic phase dependence across the whole field-of-view. We interpret this as a so far unidentified systematic effect in the *Kepler* data. We discuss the presence of regular patterns in the distribution of multiple periodicities and amplitudes. In the period-amplitude plane we find that it is possible to distinguish between solar-like oscillations and larger amplitude pulsations which are characteristic for Mira/SR stars. This may indicate the region of the transition between two types of oscillations as we move upward along the giant branch.

Key words: stars: variables: general – stars: AGB and post-AGB – techniques: photometric

1 INTRODUCTION

M giants are long period variables requiring years of continuous observations for their study. Much of our recent knowledge was gained from microlensing surveys of the Magellanic Cloud and the Galactic Bulge, such as MACHO (Wood et al. 1999; Alard et al. 2001; Derekas et al. 2006; Fraser et al. 2008; Riebel et al. 2010), OGLE (Kiss & Bedding 2003, 2004; Ita et al. 2004; Soszyński et al. 2004, 2005, 2007, 2009, 2011, 2013) and EROS (Lebzelter et al. 2002; Wiśniewski et al. 2011; Spano et al. 2011).

While analysing photometric data of red giants in the MACHO survey of the LMC, Wood et al. (1999) found several sequences in the period-luminosity (P-L) plane, which were labelled as A, B, C, E and D representing shorter to longer periods, respectively. Subsequent studies have shown that the structure of the sequence is rich with over a dozen features that have a luminosity (below or above the tip of the Red Giant Branch - see, e.g., Kiss & Bedding 2003; Fraser et al. 2008) and chemical composition (carbon-rich vs. oxygen-rich, Soszyński et al. 2009) or migth have a dependency on the wavelength range of the luminosity indicator (Riebel et al. 2010). The most distinct parallel sequences A and B represent the radial overtone modes of semiregulars (SR). They are numerous and most of them have multiple periods. The Miras lie on sequence C which corresponds to the fundamental mode (Wood et al. 1999; Xiong & Deng 2007; Takayama et al. 2013). The

power spectra of semiregulars that are observed for a large number of pulsation periods show modes with solar-like Lorentzian envelopes. This suggests that stochastic excitation and damping take place. With decreasing luminosities the pulsations decrease in amplitude and become more difficult to detect. However, these also have shorter periods, making them good candidates for space photometry from *CoRoT* and *Kepler*, giving high-quality light curves for their analysis. In addition to the mentioned sequences of the SRs and Miras, there are two sequences in the P-L plane: sequence E and D representing the eclipsing binaries and the Long Secondary Periods, respectively (Wood et al. 1999). The latter remains unclear for a host of reasons (Nicholls et al. 2009; Wood & Nicholls 2009; Nie et al. 2010).

Although there is significant improvement in the understanding of M giant variability, there remain many question regarding the excitation and damping of the pulsations, the interplay of convection and the kappa-driven oscillations and the expected crossover from Mira-like to solar-like excitation (Dziembowski et al. 2001) which must take place in M giants. While the period-luminosity relations seem to be universal regardless of the galactic environment (see Tabur et al. 2010), the full potential of these stars as tracers of the galactic structure is still yet to be fully explored. The presence of many frequencies of oscillations is expected to enable the application of asteroseismology for the most luminous giants that may be affected by the mass-loss in the upper parts of the giant branch. There has also been some controversy on the short-period microvariability of Mira-like stars (de Laverny et al. 1998; Woźniak et al. 2004; Lebzelter 2011), for which *Kepler* might prove to be ideal for resolving the issue. The complex light curves have also been interpreted in terms of stochasticity and chaos (Kiss & Szatmáry 2002; Buchler et al. 2004; Bedding et al. 2005). The hundreds of cycles for the shortest-period M giants will allow for the testing of these phenomena

Working Group 12 (hereafter WG12) of the Kepler Asteroseismic Consortium (Gilliland et al. 2010) was formed for the purpose of studying Mira and Semiregular pulsations in the *Kepler* data. Here we present the first results obtained from the analysis of the WG12 sample. The paper is organised as follows. Sec. 2 presents a detailed description of the WG12 stars, which indclude the selection criteria. Sec.3 describes the data analysis. Sec. 4 presents the comparison of our results with ground-based photometry, study of frequencies and amplitudes of light-curve variations and time-frequency analysis. A brief summary is given in Sect.5.

2 THE WG12 SAMPLE AND ITS *KEPLER* OBSERVATIONS

M giants are the longest period variable stars in the KASC program, studied within WG12. The typical time-scale of variability is in the order of one or two Kepler quarters, which means removing instrumental drifts is very difficult. On the other hand, their amplitudes are above the usual instrumental effects, so correcting for the M giant light curves should be a relatively simple task (and hence essentially neglecting every systematics that go beyond a constant vertical shift in the light curves from quarter to quarter). After having combined three years of *Kepler* data (we used the quarters Q0 − Q12), we can characterize M giant variability in a homogeneous and meaningful way.

The total sample includes over 300 M giant stars. We had two lists of targets: one was initially selected from a dedicated northern ASAS3 variability survey of the Kepler field (Pigulski et al. 2009),

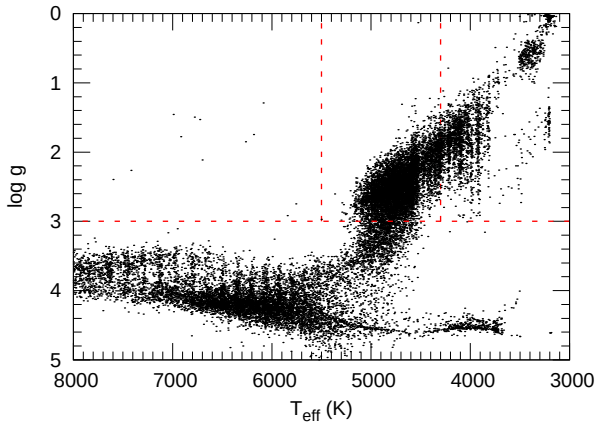

Figure 1. Surface gravity vs. effective temperature from the Kepler Input Catalogue (KIC). Stars with KIC magnitude < 12 are plotted. The bright K giants are confined between the two red vertical dashed lines, while the M giants were selected from the upper right region.

while the second one was a control sample using the Kepler Input Catalogue (Koch et al. 2010). M giant targets have been selected by combining $T_{\rm eff}$ and $\log g$ values from KIC10, the J−K colour from 2MASS and the variability information from the ASAS3 survey. We adopted $T_{\rm eff} < 4300$ K, $\log g < 3.0$ and restricted the sample to Kepler magnitude < 12 (see in Fig. 1). A cross-correlation with ASAS3 resulted in 317 stars, which were further cleaned by removing problematic cases (e.g., crowding index < 0.95 or an ASAS3 variability that is incompatible with a red giant). That has resulted in 200 targets with variability information. Since the ASAS3 variables are all cooler and larger amplitude stars, we created a supplementary list of further 200 target candidates with hotter M giants randomly selected from KIC10 with the same limits ($T_{\rm eff} < 4300$ K and $\log g < 3.0$). These stars are expected to show small-amplitude pulsations that were not detectable with the ASAS3 survey. The final list of targets that was approved for observations by *Kepler* contained 198 stars from the ASAS3 variable list and 119 from the control sample list. Most of these 317 stars have uninterrupted long-cadence (one point per every 29.4 points and short gaps between the quarters) coverage throughout Q0 to Q12 and their data were analysed using the process described below.

3 DATA ANALYSIS

3.1 Correcting M giant light curves

The *Kepler* space telescope rolls 90 degrees every quarter of a year, and consequently, variability of the majority of target stars is measured by a different CCD camera every quarter in a cycle of a year. For M giants with variability time-scales comparable to the quarter year length time-scale, there is great difficulty separating quarter-to-quarter variations from the intrinsic stellar variability (Gilliland et al. 2011).

Fig. 2 presents raw light curves of eight stars showing the gaps in the data. Clearly, some of the light curves (e.g. KIC 6279696, KIC 7274171) have smaller gaps and are more smoothly connected than others (e.g. KIC 4908338, KIC 11768249). Given the wide range of the frequency and the magnitude of the variations of the targets, it is not possible to use the same method with the same parameters for correcting the gaps for all stars because blind stitching

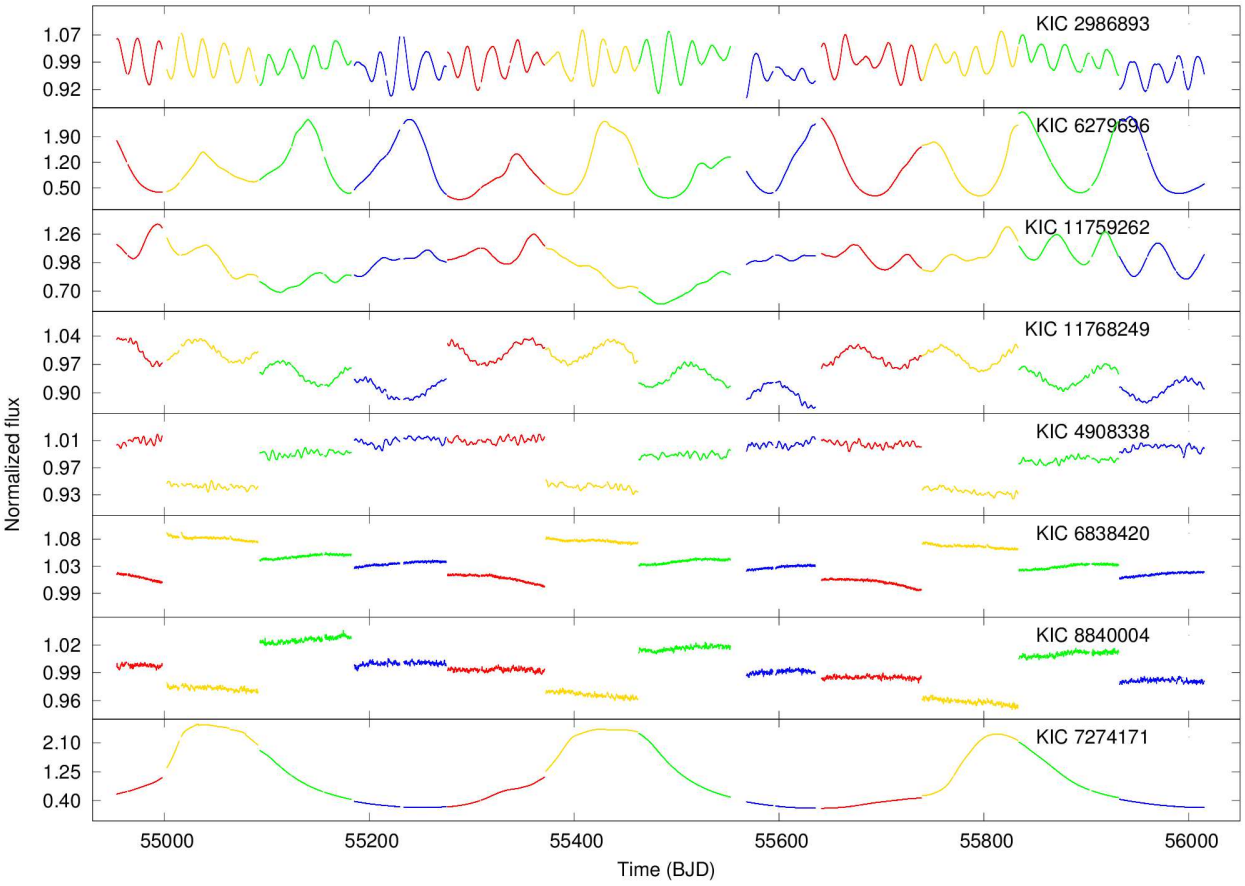

Figure 2. Light curves of various M giants emphasising flux jumps of stars with different light variations. (See the electronic version of the article for the figure in colours.)

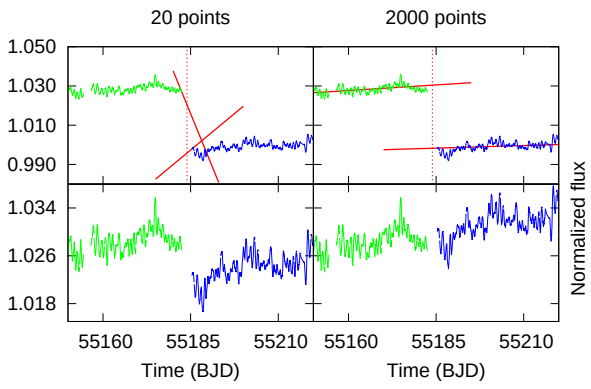

Figure 3. An example for the dependence on the number of points selected for the linear fits when correcting for the quarter-to-quarter jump.

can lead to even more discontinuous light curves. Furthermore one or more quarters are missing there is no a unique solution.

García et al. (20110) discussed in great details how KASC targets (solar-like oscillators, classical pulsating stars, lower luminosity red giants) have been corrected for outliers, jumps and drifts in the data, that have been caused by many different reasons. Most importantly, the rotation of the telescope introduces a quasi-regular cycle of systematic jumps in the mean flux, reflecting the fact that the pixel mask used for photometry does not capture all the flux. Pixels with low signal were deliberately discarded, which was good for transit detection but made absolute photometry impossible on long time scales. García et al. (20110) described the processing procedures developed for correcting the light curves that are optimised for the asteroseismic study of solar-like oscillating stars. While whose procedures work perfectly for the rapidly oscillating stars, they were essentially limited to stellar variability time scales shorter than 10 days.

Kinemuchi et al. (2012) also discussed several general methods for correcting the flux jumps between the quarters. One proposed method is to align the time-invariant approximations for crowding and aperture flux losses. A caveat of this method is that the correction factors are model-dependent and are averaged over time, whereas in practice they do vary from time-stamp to time-stamp. Another possibility is to normalize each light curves by a functional fit or a statistical measure of the data. However, this method might introduce non-physical biases into the data. The third method is to increase the number of pixels within the target mask,

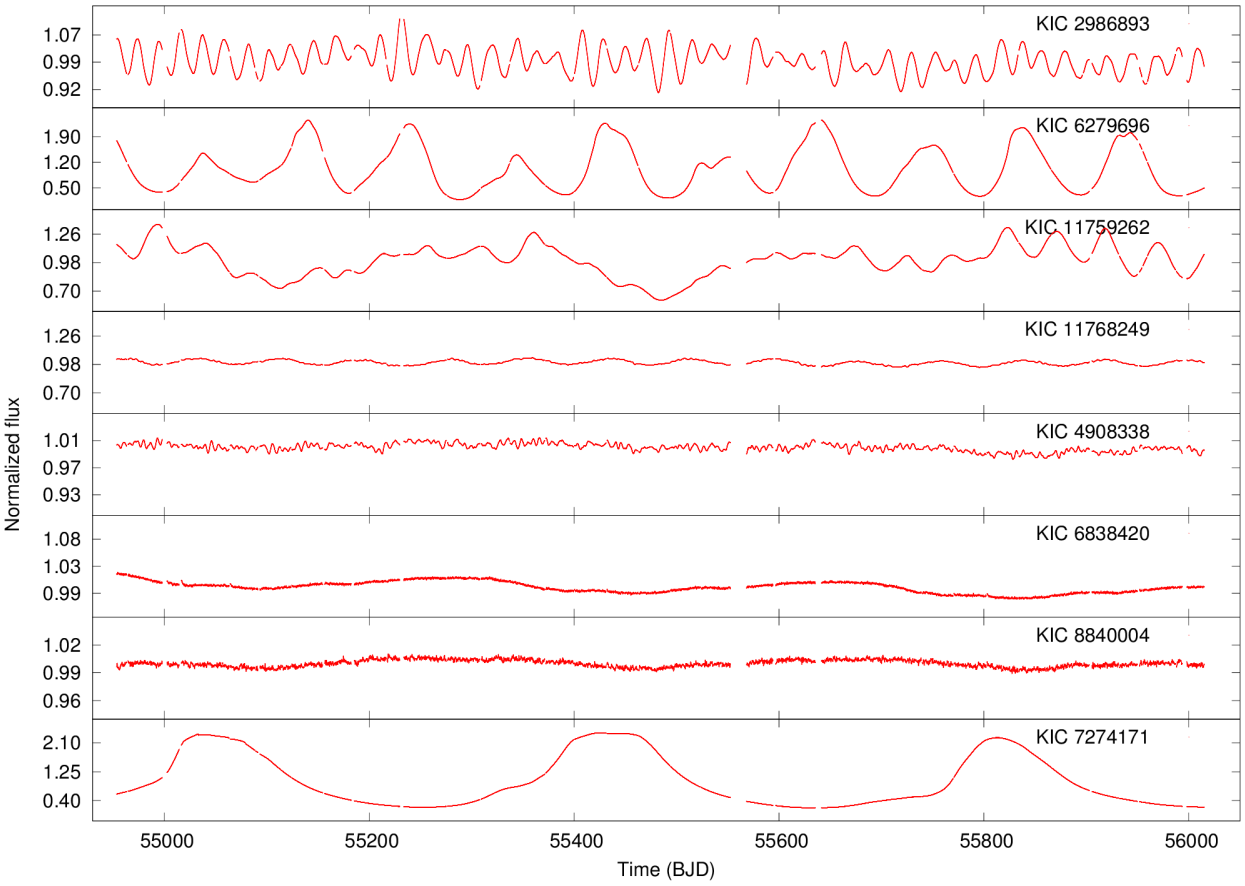

Figure 4. Data for the same stars as in Fig. 2 after the correcting procedure.

although this will introduce additional shot noise into the resulting light curve.

The above mentioned methods are best-suited for rapid variables or transiting exoplanet systems, where a smooth averaging does not distort the stellar signal. Furthermore, for an M giant where the length of the quarter is comparable to the mean timescale of variability, we should avoid methods that are otherwise perfect for other types of stars. Because of that, we decided to follow a simple procedure to correct for the flux jumps only and have all the low-frequency signals (both stellar and instrumental) untouched. Linear fitting and extrapolation for correcting the gaps between the quarters were used to optimize the quarter-to-quarter offsets for obtaining the most smoothed shape possible. For each light curve and a selected gap we fit a line to a selected number of points before the gap and fit another to a selected number of points after the gap. Next,we extrapolate both of the fitted lines into the center of the gap. The difference between the two lines represents the amount of shift required for a smooth transition between the two adjacent quarters, with which the flux data in the later quarter was multiplied.

We have developed a graphical user interface (GUI), which allows the user to set easily the fitting parameters for the program calculating the shifts. The fitting parameters include setting the number of points to be used for the linear fits with the option of setting the number of points for all quarters or quarter by quarter. For light curves that did not contain rapid brightness changes 20 points were used for the fit, whereas for light curves that were dominated by high frequency variation 2000 points were (in the latter the linear fit averaged out the rapid fluctuations but retain the information of the slow trends). For some light curves different quarters required different sets of fitting parameters, predominantly when a quarter was missing. The stitching program makes a log of the used parameters, and includes it in the output file as a header. We applied the above mentioned procedure the entire collection of 317 stars of our sample, visually inspecting the light curves and adjusting the fitting parameters for each case. Fig. 3 shows an illustration of why identical fitting parameters were impossible to use: while 20 points were usually perfectly enough for getting a smooth transition between two quarters, stars with rapid fluctuations must be treated differently.

Figure 4 presents the light curves of the same eight stars that were plotted in Fig. 2, after correcting for the gaps with our code. The program also normalises the data by the mean flux level. In the case of KIC 4908338, KIC 6838420 and KIC 8840004 we used 2000 points for the fits, 20 points were used for KIC 2986893 (ex-

cept for the gap around BJD 55500)[1], KIC 6279696, KIC 7274171 and KIC 11759262, while the dataset for KIC 11768249 was corrected with linear fits to 200-200 points neighbouring the gaps. Note that each of these light curves contains approximately 48,000 points.

All the corrected WG12 data analysed here are available for download through the electronic version of this paper.

3.2 Methods of analysis

To characterise M giant variability with *Kepler*, we have performed several simple analyses. We compared the data to ground-based observations where possible, then studied the amplitudes and periodicities with standard approaches. Finally, we looked into the time-dependent changes of the periods and amplitudes using the time-frequency distributions.

To demonstrate the potential and properties of the data, we carried out several comparisons with ground-based photometric observations such as those of the American Association of Variable Star Observers (AAVSO) or the All Sky Automated Survey (ASAS).

Amplitude and periods were determined from the Fourier transform of the time series with the program `Period04` (Lenz & Breger 2005). Amplitudes and periods were determined from the Fourier spectra calculated with `Period04`. In order to study the time dependent phenomena, e.g. amplitude and frequency modulation, mode switching, etc. we calculated time-frequency distributions for all stars using the weighted wavelet-Z transform code (WWZ, Foster 1996).

4 DISCUSSION

4.1 The *Kepler*-year in the data

The first visual inspection of the data revealed an interesting group of stars with similar variability. We first considered this group as rotationally modulated stars. However, a closer investigation of their periods and phases indicated that those changes are likely to be caused by a so-far unrecognised systematics in the *Kepler* data. For 56[2] stars we found small variations with sinusoidal modulation and period similar to the *Kepler*-year (372.5 days). This is demonstrated in Fig. 5. This small amplitude fluctuation became clearly noticeable only now, after three years of data collection. It remains unnoticeable in the light curves of Mira and semiregular stars due to their large amplitudes.

To our knowledge, no *Kepler* Data Release Notes mention this periodicity as an existing systematic effect in the data. Likely this trend has gone unnoticed because in most science investigations using *Kepler* data the light curves are flattened (e.g. exoplanet studies, asteroseismology of solar-like stars or low-luminosity red giants), so that intra-quarter variability was left unexplored. For M giants bridging many quarters by their intrinsic variability, the possibility of a new systematic effect cannot be neglected. To check whether this is indeed the case, we performed a detailed investigation into the amplitude and phase dependence of the *Kepler*-year signal across the total field-of-view.

[1] In several cases the gap after the 7th quarter needed more points for the fit, because it was caused by a safe mode event and lasted 16 days as opposed to the ordinary 2 days.

[2] 56 out of 241 stars. If there were any missing quarters it was not possible to securely determine the presence of the *Kepler*-year

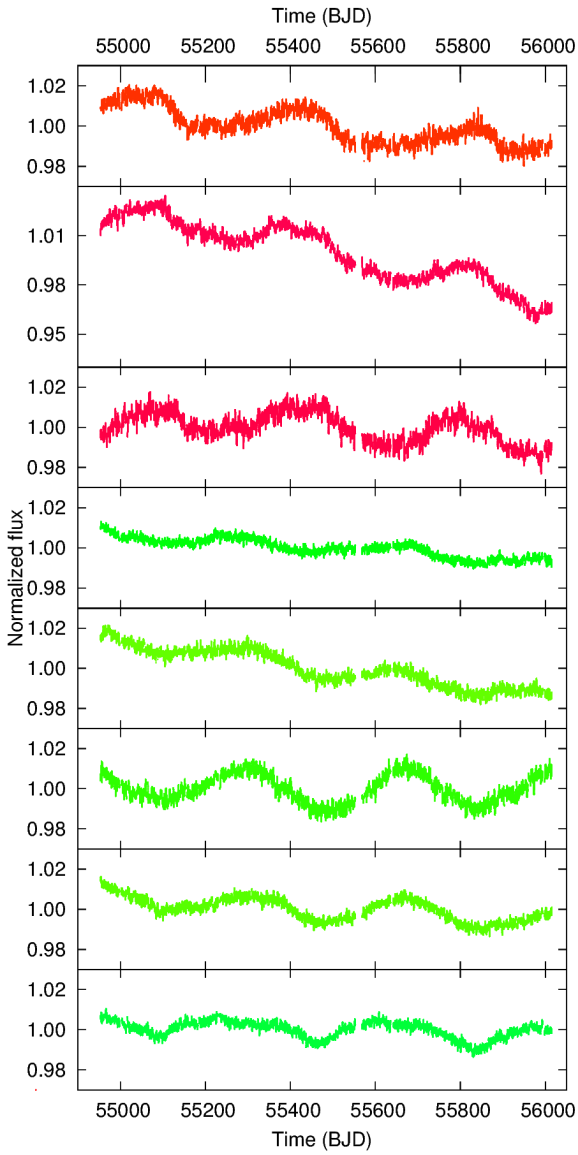

Figure 5. Examples for the three-wave light curves. Colours are indicating the phase of the *Kepler*-year. Note the apparent alternation of the red (top three) and green (bottom five) light curves. (See the electronic version of the article for the figure in colours.)

The phase of the *Kepler*-year wave scatter quite a lot in the group of these stars. However, Fig. 5 nicely illustrates that in broad terms the three-wave light curves can be divided into two groups, in which the maxima and the minima of the signal are alternating (see, for instance, the local maxima in the upper three panels and the local minima in the lower five panels at around BJD 55450). We have searched the positions of the stars in the CCD-array and noticed that there is a clear correlation between the phase behaviour and the location in the field. This is shown in Fig. 6, where the colour-codes indicate the actual phase of the signal with an arbitrary zero-point. Apparently, the figure is dominated by the green and red colours, most red dots located in the center and the green ones near to the edge.

In conclusion, one has to be careful when using *Kepler* data

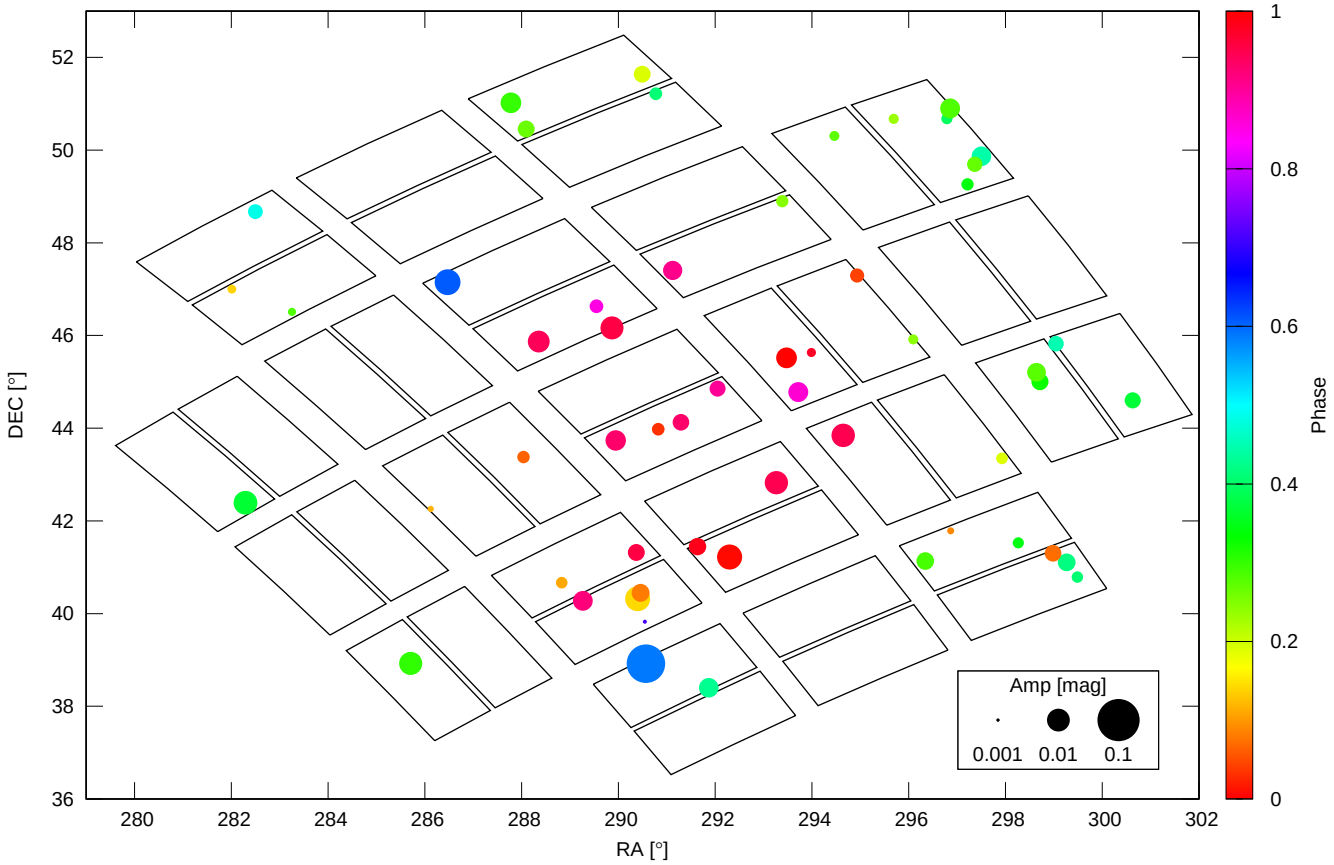

Figure 6. Positions of the stars with the *Kepler*-year signal in the FOV. The colour bar shows the phase of the wave with an arbitrary zero-point. The size of the dots indicates the amplitude of the wave. (See the electronic version of the article for the figure in colours.)

for investigating very long-term phenomena, such as M giant pulsations or stellar activity cycles, or any other study that needs homogeneous and undistorted data over many hundreds of days. The typical amplitude of the *Kepler*-year signal is around 1 percent, which is way above the short-term precision of the data. We are currently exploring if this systematic effect can be removed by pixel-level photometry (Bányai et al., in prep.).

4.2 Comparison with ground-based photometry

We compared *Kepler* measurements with ground-based photometry provided by the ASAS and AAVSO databases. In this section we use AAVSO data (visual, photoelectric V and RGB-band Digital single-lens reflex (DSLR) data) to study how well can the ground-based and space data be cross-calibrated.

For three well-known long-period variables we compared the AAVSO and *Kepler* light curves and their frequency spectra. In Fig. 7 we overplotted ten-day means of AAVSO visual observations and *Kepler* data for the semiregular variable AF Cyg. Here the *Kepler* data were converted from fluxes to magnitudes via the usual $\mathrm{mag} \sim -2.5 \log(\mathrm{flux})$ and zero-points matched for the best fit. We found that although the shape of the two curves are very similar for the all three stars, a better fit can be achieved when the *Kepler* magnitudes were further scaled by a multiplicator of 1.6-

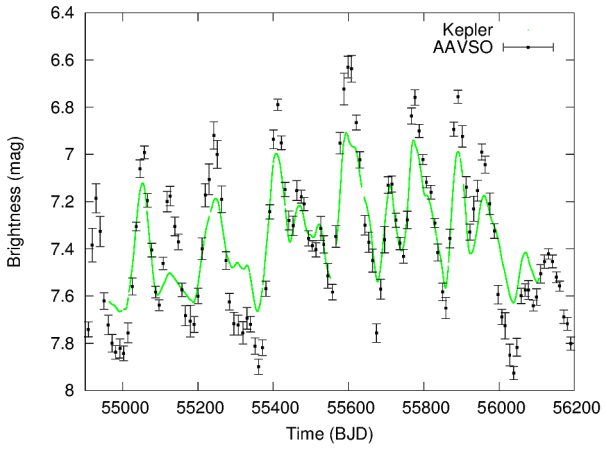

Figure 7. AF Cyg AAVSO and *Kepler* light curves before scaling *Kepler* data to AAVSO.

2.4. The scaled *Kepler* and AAVSO light curves are plotted in Fig. 8. The two sets of light curves are very similar after a simple scaling, even though the photometric bands were very much different.

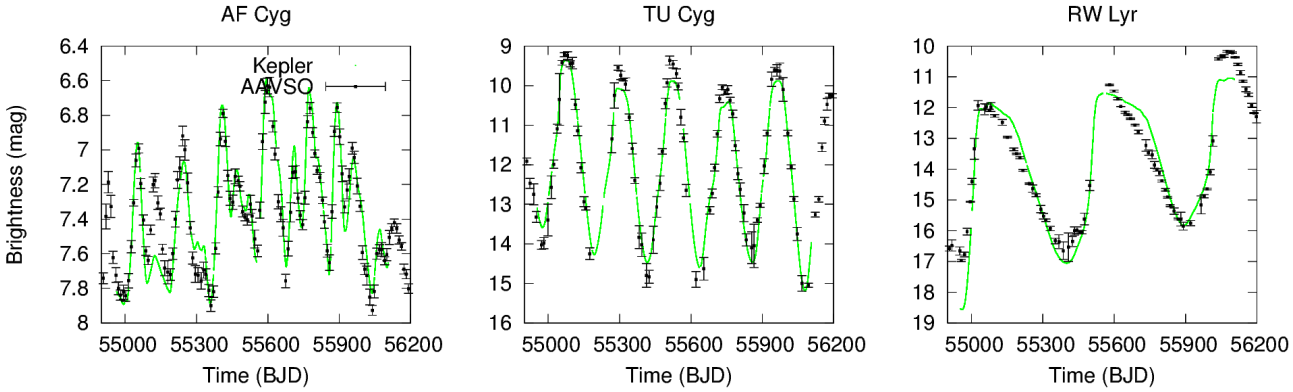

Figure 8. A comparison of AAVSO and the scaled Kepler light curves for three well-known long-period variables – AF Cyg, TU Cyg, RW Lyr –, based on AAVSO and the scaled *Kepler* light curves. In panels (a) and (b) the AAVSO data are 10-day means of visual observations; in panel (c) the brightnesses came from average measurements in Johnson V and the green channel of RGB DSLR observations. Black squares are the AAVSO data with error bars, the green dots correspond to the *Kepler* data.

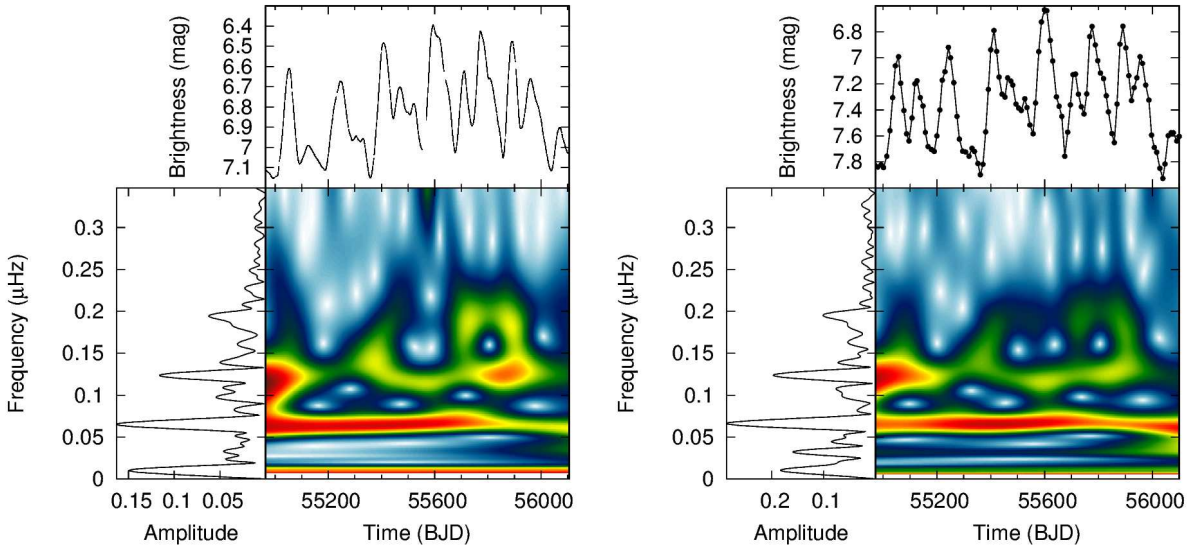

Figure 9. *Left:* the wavelet map of AF Cyg from the *Kepler* light curve. *Right:* the same from the AAVSO light curve.

The wavelet maps of AF Cygni (Fig. 9) are also very similar, with only minor differences in the amplitude distribution.

To characterise periodicities we performed a Fourier analysis for all the corrected light curves. With subsequent pre-whitening steps we determined the first 50 frequencies with `Period04`. In many cases, there were only a couple of significant peaks (like for AF Cyg), while for the lower-amplitude stars even 50 frequencies may not include everything that can be extracted from the data.

The general conclusion based on the various comparisons to ground-based data is that there is a good correspondence between the two data sources in terms of the dominant periods and the shape of the light curves for the high-amplitude long-period variables. *Kepler*'s unique precision allows the determination of more periods for the lower-luminosity stars, but in cases when the frequency content is simple (like for a Mira star or a high-amplitude semiregular variable), 1,100 days of *Kepler* data are still too short for revealing meaningful new information. However, the uninterrupted *Kepler* curves shall allow the detection of any kind of microvariability with time-scales that are much shorter than those of the pulsations. We note here that we found no star with flare-like events that would resemble those reported from the Hipparcos data by de Laverny et al. (1998).

4.3 Multiple periodicity and amplitudes

The light curves of M giant variables can be very complex, seemingly stochastic with one or few dominant periodicities. The complexity is inversely proportional to the overall amplitude: while large amplitude Miras are known to be singly periodic variables with coherent and stable light curves, the decreasing amplitude is typically associated with complicated light curve shapes that can be interpreted as a superposition of multiple frequencies that correspond to different pulsation modes. The *Kepler* WG12 sample,

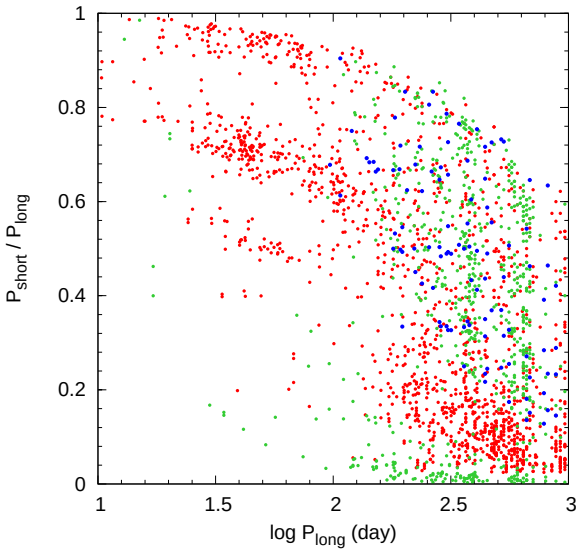

Figure 10. Petersen-diagram using the first five periods for each star. Red dots refer to the ASAS group, green dots to the the control sample and blue ones to Miras. (See the electronic version for the article for the figure in colours.)

consisting of two subsamples, one selected by variability and one control sample based on their estimated physical parameters, shows many features in the distribution of amplitudes and periods that were found previously in other, ground-based surveys. Here we attempt to characterise the systematic distinction between different groups of stars.

Based on the complexity in the time and the frequency domains, we sorted the stars into three groups. Stars in Group 1 have a wide range of periods between a few days and 100 days (e.g. KIC 4908338 or KIC 11759262 in Fig. 4). Group 2 contains stars with very low-amplitude light curves that are mostly characterised by very rapid changes (e.g KIC 6838420, KIC 8840004 in Fig. 4), occasionally supplemented by slow changes that may be related to rotational modulation or instrumental drifts. A close inspection showed that all of them belong to the control sample. Stars with light curves containing only a few periodic components (as Miras and SRs) compose Group 3 (e.g. KIC 7274171 in Fig. 4). In the rest of the paper we refer to these stars as Group 1, Group 2 and Group 3, even though there is a one-to-one correspondence between the ASAS and the control sample.

Similarly to previous studies (e.g. Soszyński et al. 2004; Tabur et al. 2010), we made a Petersen diagram (period ratios vs. periods) for all WG12 stars to check any regularity in the frequency spacing and ratios. To make the diagram, we took the five most significant periods and selected every possible pair to plot their ratio as a function of the longer of the two. In Fig. 10 we plotted each groups with different colours. The most apparent structure is seen between $\log P = 1$ to $\log P = 2$, where the predominantly ASAS sample (Group 1, red dots) is clearly separated into several concentrations of points at well-defined period ratios. The mostly populated clump is around $P_{\rm short}/P_{\rm long} \approx 0.7-0.8$, a ratio that is known to belong to the upper Red Giant Branch stars, one to two magnitudes below the absolute magnitude of the Tip of the Red Giant Branch (TRGB, see Kiss & Bedding 2003, 2004). The ratio is in excellent agreement with the analysis of period ratios for a similar-sized sample

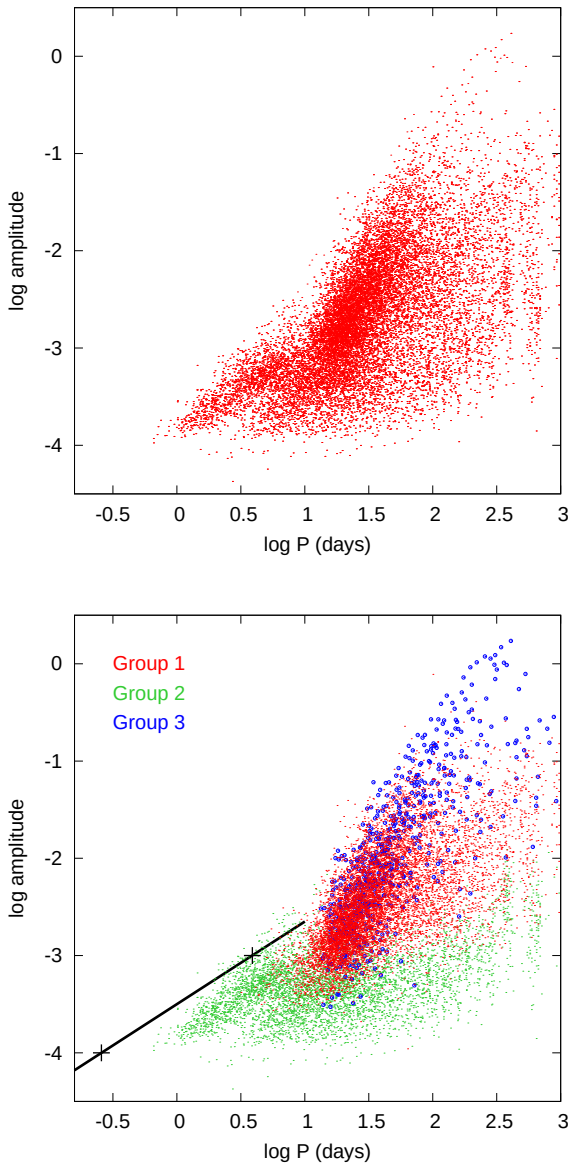

Figure 11. We plotted the period-amplitude relations for the whole sample on the top panel. On the bottom panel we used different colours to distinguish between the three groups. Plus signs refer to two selected points in the top panel of Fig. 3. of(Huber et al. 2011) related to solar-like oscillations, back line is drawn through these points. (See the electronic version of the article for the figure in colours.)

of bright southern pulsating red giants by Tabur et al. (2009) and those in OGLE observations by Soszyński et al. (2004).

Traditionally, this ratio has been interpreted as due to pulsations in the first and second radial overtone modes in theoretical models (e.g. Wood & Sebo 1996). Recently, Takayama et al. (2013) performed detailed modelling of OGLE Small Amplitude Red Giants (OSARGs) from the OGLE-III catalogue (Soszyński et al. 2009), for which they found that the rich structure in the OSARG Petersen diagram can be explained by radial overtone modes, as well as with non-radial dipole and quadropole modes. Our plot in Fig. 10 lacks the details of the sub-ridges that are so easily visible in the OGLE-III data - partly because of the lower number of stars,

partly because of the significantly shorter time-span of the *Kepler* observations.

Another significant concentration is seen for period ratios close to 1 (usually between 0.9 and 1). As has been pointed out several times in the literature, closely spaced periods in red giants can be explained by several possible mechanisms, including two closely separated oscillation modes, high-overtone radial pulsation, a single period that changes slightly, or may be an artefact from amplitude/phase modulation (see, e.g., Benkő, Szabó & Paparo 2011, for details on the latter). Takayama et al. (2013) more or less succeeded to fit the ratios between 0.85-0.95 with non-radial third and fourth overtone modes ($l = 1$ and $l = 2$ p_3, p_4 modes), but were unable to reach over 0.95 with the considered set of modes. Our preferred explanation for the near-unity ratios is that of slight changes of a given period, a conclusion that is supported by the variations detected in the time-frequency distribution (see later in Sec. 4.5).

The third distinct clump is visible around period ratios of 0.5. This could either be related to pulsation in the fundamental and first radial overtones (Takayama et al. 2013) or to non-sinusoidal light curve shapes, for which the integer harmonics of the dominant frequency appear with large amplitudes (such as the long-period eclipsing binaries).

Looking at the location of the green points in Fig. 10, it may seem surprising that stars in Group 2, i.e. objects characterised by their rapid variability, hardly appear in the lower left corner of the plot, where the short-period variables should fall. Instead, the green points are scattered in the long-period end of Fig. 10, which means that their Fourier spectra are heavily contaminated by low-frequency noise, so that extracting only the first five peaks in the spectra is not enough to measure the frequencies of the rapid variations. This behaviour is well documented for lower-luminosity red giants, where the regular frequency pattern of solar-like oscillations appear on top of the granulation noise that rises like an inverse power-law signal in the power spectra. The lack of any structure in the green points in Fig. 10 (except the vertical concentration at $\log P = 2.57$ corresponding to the *Kepler*-year) confirms the noise-like behaviour for Group 2.

The few blue points for Group 3 stars in Fig 10 do not reveal any significant structure, although they appear close to the extensions of the distinct clumps of the red points. This is expected from the similar behaviour of larger amplitude AGB variables in the Magellanic Clouds.

For further investigations into the nature of the three Groups, we studied the amplitudes and their distributions. First we made the period-amplitude plot for the whole sample, using all the 50 frequencies and amplitudes calculated by `Period04`. This is shown in the upper panel of Fig. 11, where the presence of two distinct populations in very much evident. The bulk of the giants are spread in a triangular region, starting at $\log P \approx 0.5$ and $\log \mathrm{amp} \approx -4$ with a very well defined upper envelope pointed to the upper right corner of the plot. To the left of this upper envelope there is a distinct feature that lies between $\log P = 0$; $\log \mathrm{amp} = -4$ and $\log P = 1$; $\log \mathrm{amp} = -3$ and indicates a good correlation between the period and amplitude. This correlation resembles the $\nu_{\max}$-amplitude scaling relation that has been extensively studied with *Kepler* data from the main sequence to red giants (e.g. Huber et al. 2011).

In the bottom panel of Fig. 11 we show the three groups with different symbols. Apparently, Group 2 populates the low amplitude part of the diagram, covering both the short-period correlation and the long-period range below Group 1 and Group 3. To validate that the correlation is indeed in the extension of the $\nu_{\max}$-amplitude relation for the solar-like oscillations, we added two points, marked by the large plus signs, and a line drawn through these points and extending it up to $\log P = 1$. The extra points refer to two selected middle points in the top panel of Fig. 3 of Huber et al. (2011), where the oscillation amplitude vs. $\nu_{\max}$ is shown for their entire Kepler sample. We selected the $A = 1000$ ppm and the $A = 100$ ppm amplitude levels, which have a mean $\nu_{\max}$ values of about 3 μHz and 45 μHz, respectively. The $\nu_{\max}$ values were converted to periods in days for the comparison. It is apparent in the lower panel of Fig. 11, that the $\nu_{\max}$-amplitude scaling goes very much parallel to th period-amplitude relation, essentially defining the upper envelope of the green points in the lower-left corner. The amplitudes measured here are about a factor of two below the line, which is an acceptable difference given the much more sophisticated amplitude measurement technique in Huber et al. (2011) that is based on previous work by Kjeldsen et al. (2008). It is interesting to note three issues here. First, our period determination was not aimed at measuring $\nu_{\max}$ at all. The fact that the blind period determination leads to a recognizable detection of the amplitude vs. $\nu_{\max}$ scaling indicates that the frequency range of the excited solar-like modes is quite narrow, hence any period with an outstanding amplitude falls close to $\nu_{\max}$. Second, there is a quite sharp ending of the clear correlation at $\log P \approx 1$ (which corresponds to 1.2 μHz). This may explain that for longer periods, the break in the upper envelope may be an indication of different kind of excitation that leads to Mira-like pulsations further up along the giant branch. The transition between the two types of oscillations seems to occur at $\log P \approx 1$ in Fig. 11, where the green dots appear in both distinct distributions of the amplitudes. Finally, for the longer period stars (red and blue points), the upper envelope of the distribution is similar to that found for bright pulsating M giants by Tabur et al. (2010, - see their Fig. 15), indicating that the *Kepler* amplitudes can also be very well compared to ground-based observations.

4.4 Power spectra

In this Section we present typical power spectra for the three Groups of the WG12 sample. The reason for this is to illustrate the rich variety of the spectra, which indicates the complexity of M giant variability.

We show spectra for four stars in each Group in the three columns of Fig. 12. It can be seen that in Group 1 the stars show a remarkable variety in the spectra, and most of the stars are characterized with several (up to 10-15) significant frequencies (we used the S/N calculator of `Period04` to quantify the significance of each peak, following the method of Breger et al. (1993). As can be seen in the middle column of Fig. 12, Group 2 stars are indeed typical solar-like oscillators with a granulation noise strongly rising below 0.2 c/d and a distinct set of significant peaks. Note that the four panels in the middle column were sorted from top to bottom by the increasing average frequency of the acoustic signal (roughly corresponding to the classical $\nu_{\max}$). Here every spectrum contains very high peaks (in relative sense) between 0 and 0.004 c/d. Peaks near 0.00267 c/d correspond to the *Kepler*-year and they appear in almost every spectra with smaller or higher amplitude. Often there is another high peak near 0.0007 c/d, which is near to $1/t_{\mathrm{obs}}$, where t_{obs} is the length of the full dataset. The acoustic signal emerges at higher frequencies in form of some sort of structured peaks at lower amplitudes but still significant compared to the local noise in the spectrum.

Spectra for Group 3 are shown in the right column of Fig.

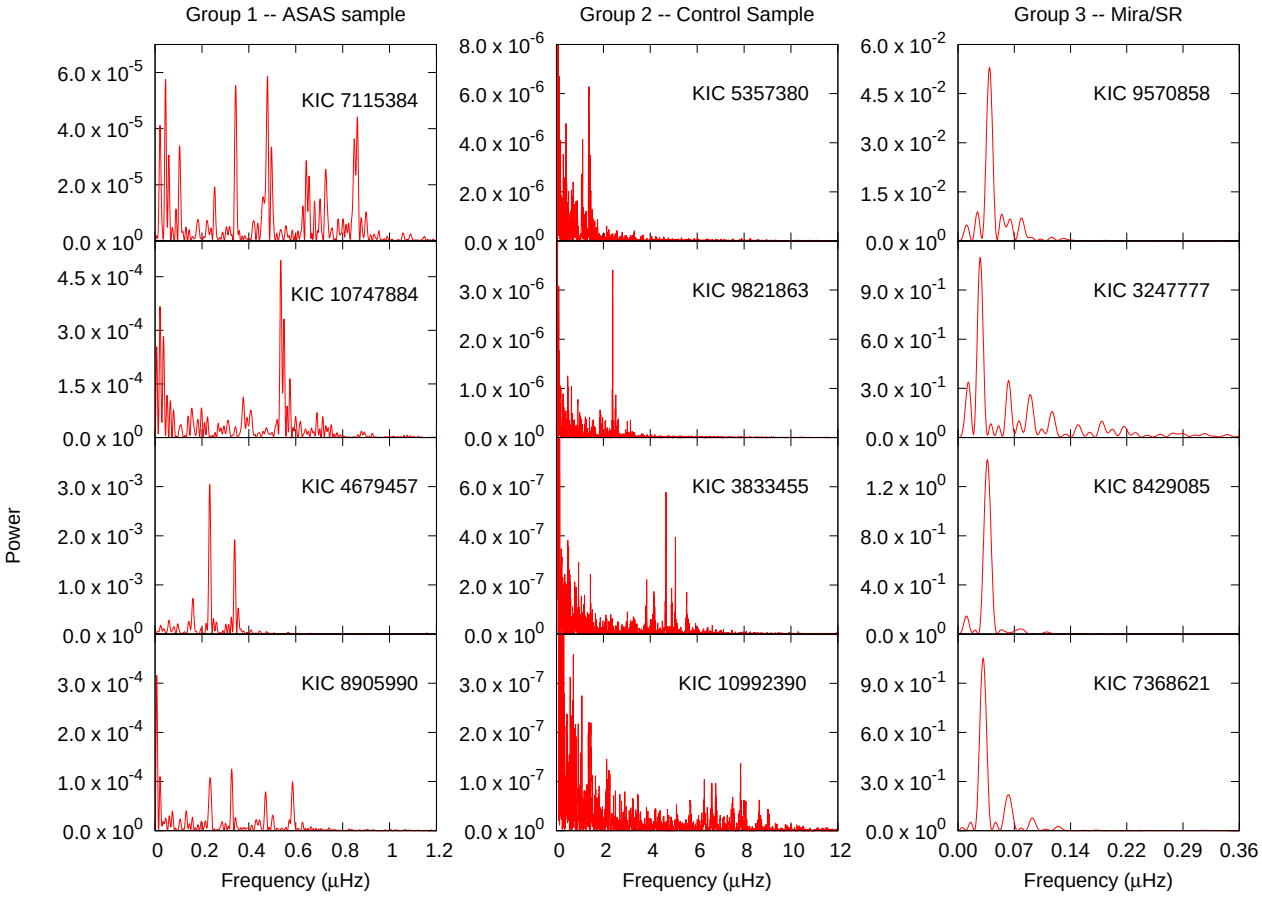

Figure 12. Typical power spectra of the three Groups

12. The highest peaks appear between 0.0025 c/d and 0.006 c/d, i.e. periods between 150 and 400 days. In some cases, we see the integer harmonics of the dominant peak, which is caused by the strong departure from the pure sinusoidal shape, characteristic for most of the Mira stars.

4.5 Time-frequency distributions

As a last step we surveyed systematically the time-frequency distributions for all stars in the three Groups. We searched for phenomena that are more difficult to detect with the traditional methods of time-series analysis, such as mode switching, amplitude modulation or frequency modulation. While a detailed study of all these phenomena is beyond the scope of the paper, we can demonstrate the typical cases in each Group.

In Fig. 13 we show three examples from each Group. The plots are organised in such a way that the wavelet map, in which the amplitude is colour-coded and normalized to unity, is surrounded by the light curve on the top and the corresponding Fourier spectrum on the left. This way we can see the temporal behaviour of the peaks in the spectrum and also in some cases the effects of gaps in the data. The three Groups were ordered in the subsequent rows from top to bottom. Group 1 stars (top row in Fig. 13) have multiperiodic light curves (P=10-50 days). The frequency content is rarely stable, most of the peaks come and go away on the time-scales of a few pulsation cycles. The amplitudes of the components change very strongly, and there is no apparent order in this. There are few cases when the strongest peaks are changing parallel to each other, like mode switching, but this is rare and difficult to distinguish from random amplitude changes.

For Group 2 stars (middle row in Fig. 13), the wavelet maps were calculated from 0.01 c/d frequency (without the long-period trends) in order to get a clearer picture of the shorter and smaller amplitude variations between 0.1-0.5 c/d, where the acoustic signal is dominant. Here the frequencies are changing even more randomly, a behaviour that naturally arises from the stochastic excitation of the solar-like oscillations. For Group 3 stars, the available time-span only allows measuring the stability of the dominant peak, in good agreement with the Mira character.

5 SUMMARY

In this paper we studied the global characteristics of light variations for 317 red giant stars in the *Kepler* database, containing 198 already known variable stars observed by the ASAS North survey and 117 stars in a control sample selected based on their estimated

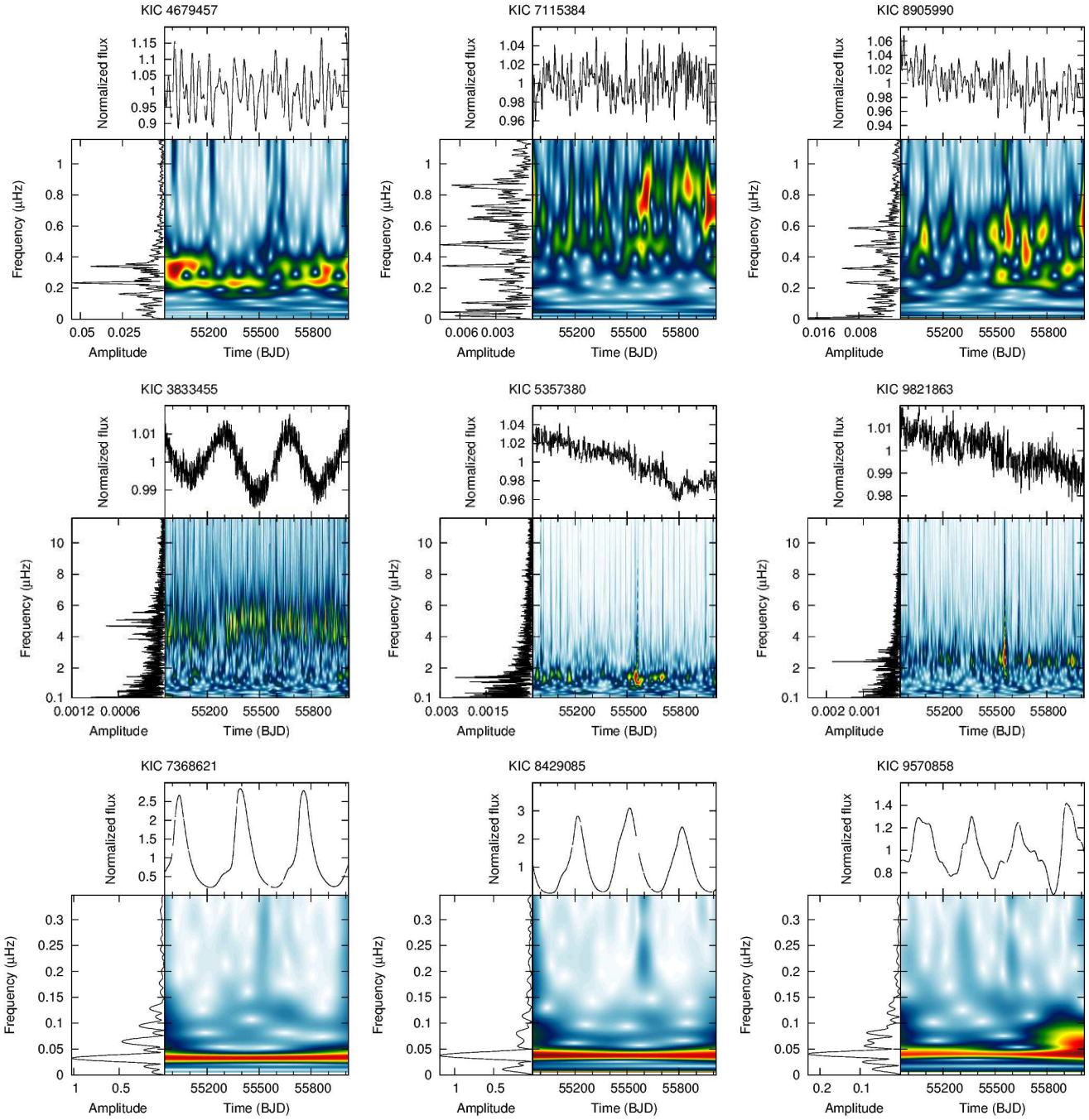

Figure 13. Time-frequency distribution for selected members of Group 1, 2 and 3 (from top to bottom). Each row contains plots for three stars in each group. The most informative cases are those for Group 1, where the wavelet maps clearly indicate that many of the peaks in the Fourier spectra (left panel in each plot) corresponds to signals that have strongly time-dependent amplitudes.

physical parameters. The main results can be summarised as follows:

(i) The study of M giants with *Kepler* poses new challenges because of the time-scale of variability that is comparable to the length of the *Kepler* quarters. Most of the usual methods for correcting the trends and jumps are thus not applicable. After extensive testing we ended up with a simple light curve stitching method, which is based on linear fits at the edges of the quarters and then matching the quarter-to-quarter shifts for creating the smoothest possible light curves. We developed a software with a user-friendly GUI, which made it easy to set the fitting parameters and stitch together each quarter. When the data contain missing quarter(s), no unique solution is possible.

(ii) Three years of observations revealed a so far unnoticed systematic fluctuation in the data, at the levels of up to 1-3%. We found that the period equals to one *Kepler*-year and the phase behaviour is clearly correlated with the position in the whole *Kepler* field-of-

view. It is not yet clear if a more sophisticated pixel photometry would be able to remove the artefact.

(iii) We compared the data with various ground based photometries (visual, ASAS CCD, AAVSO DSLR, etc.) and concluded that for the large-amplitude stars, *Kepler* light curves can be matched very well with the ground-based data, but the amplitudes require a significant scaling by about a factor of two. *Kepler*'s main advantage for these slow variables is the uninterrupted observations at high-precision and high-cadence (relative to the pulsation periods), so that secondary low-amplitude variations, unrelated to pulsations remain a task for ground-based observers who can maintain regular observations for many years or even decades.

(iv) We studied the distributions of periods, period ratios and amplitudes. There are several regular patterns in these distributions that can be explained by the presence of several pulsation modes, some possibly non-radial dipole or quadropole modes. We find evidence of a distinction between the solar-like oscillations and those larger amplitude pulsations characteristic for Mira/SR stars in the period-amplitude plane. This may show the transition between two types of oscillations as a function of luminosity.

(v) The power spectra and time-frequency distributions reveal very complex structures and rich behaviour. Peaks in the spectra are often transient in terms of time-dependent amplitudes revealed by the wavelet maps. The overall picture is that of random variations presumably related to the stochasticity of the large convective envelope.

With this paper we highlighted the global characteristics of M giant stars seen with *Kepler*. There are several possible avenues to follow in subsequent studies. Given the time-span and the cadence of the data, an interesting avenue of investigation is to perform a systematic search for rapid variability that can be a signature of mass-accreting companions. One of the archetypal types of such systems, the symbiotic binary CH Cyg, has been both KASC target and Guest Observer target, and its data can be used as a template to look for similar changes in the full *Kepler* red giant sample. Another possibility is to quantify the randomness of the amplitude changes using detailed statistical analysis of the time-frequency distributions.

ACKNOWLEDGMENTS

This project has been supported by the Hungarian OTKA Grants K76816, K83790, K104607 and HUMAN MB08C 81013 grant of Mag Zrt., ESA PECS C98090, KTIA URKUT_10-1-2011-0019 grant, the Lendület-2009 Young Researchers Program of the Hungarian Academy of Sciences and the European Community's Seventh Framework Programme (FP7/2007-2013) under grant agreement no. 269194 (IRSES/ASK). AD, RSz and GyMSz have been supported by the János Bolyai Research Scholarship of the Hungarian Academy of Sciences. AD was supported by the Hungarian Eötvös fellowship. RSz acknowledges the University of Sydney IRCA grant. Funding for this Discovery Mission is provided by NASA's Science Mission Directorate. The Kepler Team and the Kepler Guest Observer Office are recognized for helping to make the mission and these data possible.

REFERENCES

Alard C. et al., 2001, ApJ, 552, 289
Bedding T. R., Kiss L. L., Kjeldsen H., Brewer B. J., Dind Z. E., Kawaler S. D., Zijlstra A. A., 2005, MNRAS, 361, 1375
Benkő, J., Szabó, R. Paparó, M., 2011, MNRAS, 417, 974
Breger, M. et al., 1993, A&A, 271, 482
Buchler J. R., Kolláth Z., Cadmus R.R. Jr., 2004, ApJ, 613, 532
de Laverny P., Mennessier M. O., Mignard F., Mattei J. A., 1998, A&A, 330, 169
Derekas A., Kiss L. L., Bedding T. R., Kjeldsen H., Lah P., Szabó Gy. M., 2006, ApJ, 650, L55
Dziembowski W. A., Gough D. O., Houdek G., Sienkiewicz R., 2001, MNRAS, 328, 601
Foster G., 1996, AJ, 112, 1709
Fraser O. J., Hawley S. L., Cook K. H., 2008, AJ, 136, 1242
García, R. A. et al., 2011, MNRAS, 414, L6
Gilliland, R. L. et al., 2010, PASP, 122, 131
Gilliland, R. L. et al., 2011,
Huber D. et al., 2011, MNRAS, 743, 143
Ita Y. et al., 2004, MNRAS, 347, 720
Kinemuchi K., Fanelli M., Pepper J., Still M., Howell S. B., 2012, PASP, 124, 919
Kiss L. L., Szatmáry K., Szabó G., Mattei J. A., 2000, A&AS, 145, 283
Kiss L. L., Bedding T. R., 2003, MNRAS, 343, L79
Kiss L. L., Bedding T. R., 2004, MNRAS, 347, 283
Kiss L. L.; Szatmáry K., 2002, A&A, 390, 585
Kjeldsen, H. et al., 2010, ApJ, 713, L79
Koch et al., 2010, ApJ, 713, L79
Lebzelter T., 2011, A&A, 530, A35
Lebzelter T., Schultheis M., Melchior A. L., 2002, A&A, 393, 573
Lenz P., Breger M., 2005, CoAst, 146, 53
Nicholls C. P., Wood P. R., Cioni M.-R. L., Soszyński I., 2009, MNRAS, 399, 2063
Nie J. D., Zhang X. B., Jiang B. W., 2010, AJ, 139, 1909
Ostlie D.A., Cox A.N., 1986, ApJ, 311, 864
Pigulski A.; Pojmański G.; Pilecki B.; SzczygiełD. M., 2009, AcA, 59, 33
Riebel D., Meixner M., Fraser O., Srinivasan S., Cook K., Vijh U., 2010, ApJ, 723, 1195
Soszyński I., Udalski A., Kubiak M., Szymański M., Pietrzyński G., Żebruń K., Szewczyk O., Wyrzykowski L., 2004, AcA, 54, 129.
Soszyński I. et al., 2005, AcA, 55, 331
Soszyński I., 2007, ApJ, 660, 1486
Soszyński I. et al., 2009, AcA, 59, 239
Soszyński I. et al., 2011, AcA, 61, 217
Soszyński I. et al., 2013, AcA, 63, 21
Spano M., Mowlavi N., Eyer L., Marquette J.-B., Burki G., 2011, ASPC, 445, 545
Tabur V., Bedding T. R., Kiss L. L., Moon T. T., Szeidl B., Kjeldsen H., 2009, MNRAS, 400, 1945
Tabur V., Bedding T. R., Kiss L. L., Giles T., Derekas A., Moon T. T., 2010, MNRAS, 409, 777
Takayama M., Saio H., Ita Y., 2013, MNRAS, 431, 3189
Wiśniewski M., Marquette J. B., Beaulieu J. P., Schwarzenberg-Czerny A., Tisserand P., Lesquoy É., 2011, A&A, 530, 8
Wood P. R. et al., 1999, In Bertre, T. L., Lebre, A., & Waelkens, C., editors, Proc. IAU Symp. 191, Asymptotic Giant Branch Stars, page 151. Dordrecht: Kluwer.
Wood P. R., Nicholls C. P., 2009, ApJ, 707, 573
Wood P. R., Sebo K.M., 1996, MNRAS, 282, 958
Woźniak P.R., McGowan K.E., Vestrand W.T., 2004, ApJ, 610, 1038

Xiong D. R., Deng L., 2007, MNRAS, 378, 1270